

Review

# Recent Advances in Pharmaceutical Cocrystals: A Focused Review of Flavonoid Cocrystals

Jia Xu <sup>\*</sup> , Qin Shi , Yanan Wang, Yong Wang, Junbo Xin, Jin Cheng and Fang Li <sup>\*</sup>

School of Pharmacy, Jiangsu Vocational College of Medicine, Yancheng 224005, China

<sup>\*</sup> Correspondence: 18816239831@163.com (J.X.); lifang210009@163.com (F.L.)

**Abstract:** Cocrystallization is currently an attractive technique for tailoring the physicochemical properties of active pharmaceutical ingredients (APIs). Flavonoids are a large class of natural products with a wide range of beneficial properties, including anticancer, anti-inflammatory, antiviral and antioxidant properties, which makes them extensively studied. In order to improve the properties of flavonoids, such as solubility and bioavailability, the formation of cocrystals may be a feasible strategy. This review discusses in detail the possible hydrogen bond sites in the structure of APIs and the hydrogen bonding networks in the cocrystal structures, which will be beneficial for the targeted synthesis of flavonoid cocrystals. In addition, some successful studies that favorably alter the physicochemical properties of APIs through cocrystallization with coformers are also highlighted here. In addition to improving the solubility and bioavailability of flavonoids in most cases, flavonoid cocrystals may also alter their other properties, such as anti-inflammatory activity and photoluminescence properties.

**Keywords:** pharmaceutical cocrystals; flavonoids; structure–property relationships; solubility; bioavailability



**Citation:** Xu, J.; Shi, Q.; Wang, Y.; Wang, Y.; Xin, J.; Cheng, J.; Li, F. Recent Advances in Pharmaceutical Cocrystals: A Focused Review of Flavonoid Cocrystals. *Molecules* **2023**, *28*, 613. <https://doi.org/10.3390/molecules28020613>

Academic Editor: Luciana Mosca

Received: 14 December 2022

Revised: 29 December 2022

Accepted: 3 January 2023

Published: 6 January 2023



**Copyright:** © 2023 by the authors. Licensee MDPI, Basel, Switzerland. This article is an open access article distributed under the terms and conditions of the Creative Commons Attribution (CC BY) license (<https://creativecommons.org/licenses/by/4.0/>).

## 1. Introduction

Cocrystals are neutral crystalline single-phase materials that contain two or more discrete neutral molecules with different stoichiometry in a crystalline lattice through non-covalent interactions including hydrogen bonds,  $\pi$ - $\pi$  interactions, halogen bonds and van der Waals interactions [1–5]. For pharmaceutical cocrystals, at least one of the coformers is an active pharmaceutical ingredient (API), and the others are pharmaceutically acceptable ingredients [6,7]. Since the crystal structure of a cocrystal is different from any starting material, its physicochemical properties may also be different. In the pharmaceutical industry, pharmaceutical cocrystals have been applied to modify the physicochemical properties of drugs, such as solubility, dissolution rate, bioavailability, hygroscopicity, compressibility, tableability and stability [8–17]. Although some other strategies including salt formation, solvates and polymorphs have also been used to tune the physicochemical properties of drugs [18–22], cocrystals are much more attractive because they can alter the properties of drugs by designing supramolecular synth without changing the chemical structures of APIs. Cocrystals can alter the physicochemical properties of drugs because that crystal structures of cocrystals are different from APIs. Thus, the different interactions will have an effect on properties. For example, the cocrystal of caffeine and methyl gallate shows much better compaction properties than the coformers, because it exhibits flat sliding planes in the cocrystal's crystal structure, which makes the compound more prone to deformation [17]. Not only that, cocrystals are mostly stable under normal conditions and can theoretically be applied to most APIs with hydrogen bond acceptors and/or donors.

Flavonoids, belonging to the family of natural products with variable phenolic structures, widely exist in fruits, vegetables, bark, roots, grains, stems, tea, flowers and

wine [23–32], and their basic structure consists of two phenyl rings and one heterocyclic ring [33]. Generally speaking, flavonoids can be divided into two categories, namely 2-phenylchromen and 3-phenylchromen. The first category includes flavones, flavanones, flavonols, anthocyanidins and flavan-3-ols, while the second one includes isoflavones and isoflavanones [34–36]. Unlike the flavonoids mentioned above, chalcone is unique in that it lacks an oxygen-heterocyclic ring but has a 3-carbon chain that acts as a bridge connecting the two phenyl rings. The molecular structures of common flavonoids are shown in Figure 1. Since Albert Szent-Gyorgyi first reported the activity of citrus peel flavonoids in preventing scurvy-related capillary hemorrhage and fragility in 1938, more biological activities have been found in flavonoids, including anticancer, anti-inflammatory, antiviral, antioxidant, antibacterial and neuroprotective activities [37–47]. However, their unfavorable properties such as poor bioavailability largely limit their clinical applications. Cocrystallization may be a good strategy to address this issue [48], and flavonoid cocrystals have become an ever-growing field in recent years.

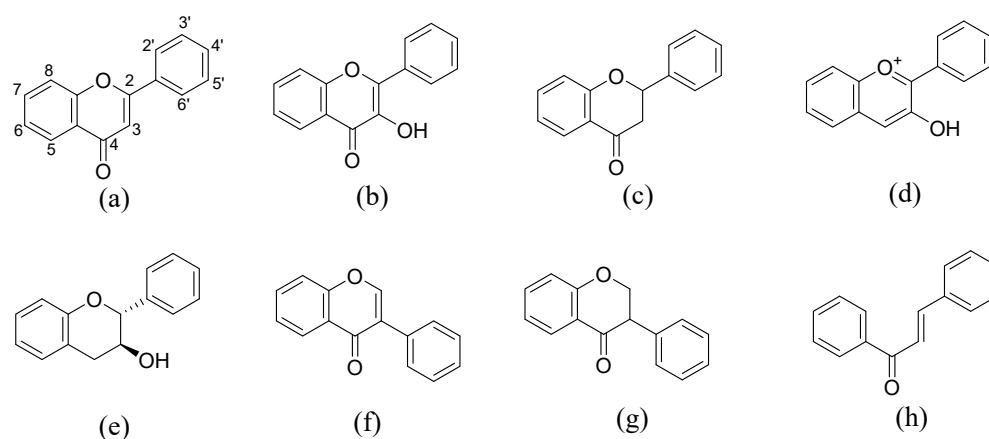


**Figure 1.** Structures of (a) flavone, (b) flavonol, (c) flavanone, (d) anthocyanidins, (e) flavan-3-ols, (f) isoflavone, (g) isoflavanone and (h) chalcone.

In this review, we not only summarize the reported flavonoid cocrystals, but also examine and analyze the interactions present in their crystal structures to find the specific interaction types and groups that are more likely to interact with the coformers. Meanwhile, the research findings of improving the solubility and bioavailability of flavonoids by forming cocrystals are introduced. Finally, we also highlight some cases in which other properties of flavonoids are regulated through cocrystallization.

## 2. Cocrystals of Flavonoids

Cocrystals of flavonoids were first reported by Daren et al. in 2008 [49]. In the study, they described four cocrystals with certain crystal structures formed by three different flavonoids and diazobicyclooctane. Since then, over 100 cocrystals have been synthesized from more than 10 flavonoids with different coformers, of which more than 60 single crystals have been cultivated. Table 1 summarizes the subclass and number of reported flavonoid cocrystals. These APIs belong to six different flavonoid subclasses, namely flavonols, flavones, flavanones, isoflavones, chalcones and dihydrochalcones, while most APIs are flavonols and flavones, which are the two largest subclasses of flavonoids. Among them, flavonols are more likely to form cocrystals; one of the reasons is that their 3-position phenolic groups tend to form intermolecular hydrogen bonds with coformers. Additionally, quercetin, one of the most studied flavonoids, has been reported to form 60 cocrystals with 22 single crystals having been solved, and its big potential to form cocrystals may be attributed to the polyhydroxy structure. Through comparison, it can be found that 12 of the 15 flavonoids have a phenolic group at the 7-position, which may be because the 7-position phenolic group is more likely to form intermolecular hydrogen bonds with the coformers. In addition, due to the different nomenclature from other sub-

classes, isoliquiritigenin and phloretin, which belong to chalcone and dihydrochalcone, respectively, have a phenolic group at the 4''-position, which is equivalent to that of other flavonoids at the 7-position. Not only that, 12 of the 15 flavonoids have a phenolic group at the 4'-position, which may also be easier to form intermolecular hydrogen bonds with cofomers. From a steric hindrance point of view, the 7- and 4'- positions are the two substituents that are most likely to interact with other molecules with the least steric hindrance. Thus, except that 3,6-dihydroxyflavone has two phenolic groups at the 6- and 3- positions, all other reported cocrystallized flavonoids have at least one phenolic group at the 7- or 4'- position. In addition, the toxicology of pharmaceutical cocrystals is also one of the important factors we need to consider. Therefore, the cofomers are usually selected from the lists of generally regarded as safe (GRAS) and pharmaceutically accepted salt formers. Since these compounds have been previously approved by the Food and Drug Administration, utilizing them for cocrystallization can reduce preclinical burden, toxicity risk and clinical trial time.

**Table 1.** Summary of reported flavonoid cocrystals.

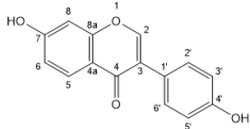
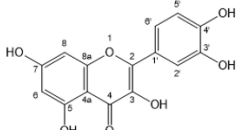
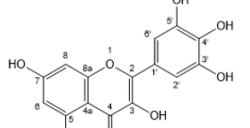
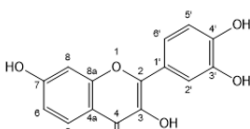
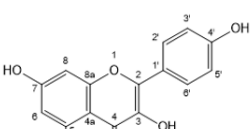
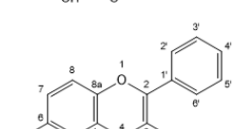
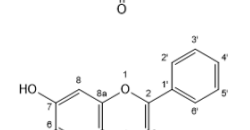
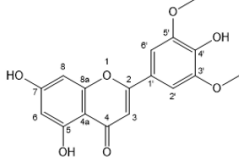
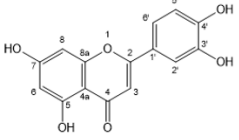
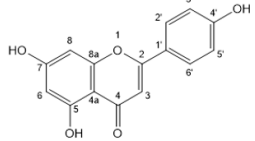
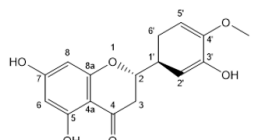
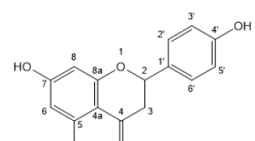
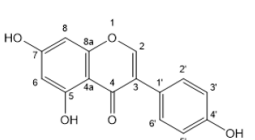
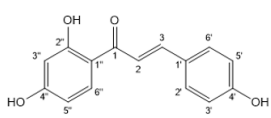
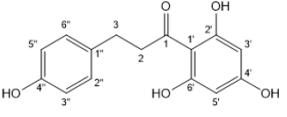
Flavonoids	Structures	Subclass	Number of Cocrystals Reported <sup>1</sup>	References
Daidzein		Isoflavones	0/1	[50]
Quercetin		Flavonols	22/60	[49,51–59]
Myricetin		Flavonols	4/8	[55,60–65]
Fisetin		Flavonols	4/4	[63,66]
Kaempferol		Flavonols	2/2	[55,58]
3,6-dihydroxyflavone		Flavonols	2/2	[49]
Baicalein		Flavones	6/8	[58,67–69]

Table 1. Cont.

Flavonoids	Structures	Subclass	Number of Cocrystals Reported <sup>1</sup>	References
Chrysin		Flavones	4/4	[58,70,71]
Luteolin		Flavones	3/3	[58,66]
Apigenin		Flavones	0/1	[50]
Hesperetin		Flavanones	5/5	[57,72]
Naringenin		Flavanones	7/9	[49,73,74]
Genistein		Isoflavones	5/5	[58,66,75–77]
Isoliquiritigenin		Chalcones	2/2	[78]
Phloretin		Dihydrochalcones	2/2	[79]

<sup>1</sup> The number of reported cocrystals with single crystals/the total number of reported cocrystals.

### 3. Structures of Flavonoid Cocrystals

According to the literature, more than 60 single crystals of flavonoid cocrystals have been cultivated. Some common features can be observed from these crystal structures. Flavonoids with a phenol group at the 5-position tend to interact with their carbonyl group at the 4-position to form an intramolecular hydrogen bond, which are common in cocrystal structures containing hesperetin, genistein, baicalein, etc. However, the phenol group at the 3-position does not interact with the neighboring carbonyl group, but dimers composed of these two groups are sometimes observed in the structures of flavonoid cocrystals, such as quercetin-4,4'-bipyridine [55], fisetin-caffeine [63], etc. The cofomers of flavonoid cocrystals also have some structural characteristics. Flavonoids tend to form cocrystals with N-containing heterocyclic compounds such as nicotinamide, isonicotinamide, theophylline,

caffeine, 4,4'-bipyridine, proline, etc. However, among these compounds, nicotinamide and isonicotinamide are most likely to be selected as cofomers, since the N-atom on their pyridine ring is a good hydrogen bond acceptor and tends to interact with the phenol group of flavonoids. This feature can also be observed in the structures of most flavonoid cocrystals whose cofomers contain a nitrogen heterocyclic ring, such as isoliquiritigenin–nicotinamide [78], genistein–caffeine [77], etc. Furthermore, amide groups containing both hydrogen bond donors and acceptors tend to interact with the phenol groups of flavonoids, which can be observed in the structures of baicalein–isonicotinamide [69], fisetin–nicotinamide [63], etc. Several typical crystal structures of flavonoid cocrystals with different features are analyzed below.

### 3.1. Quercetin–Isonicotinamide Cocrystal

The two-dimensional hydrogen bond network in the quercetin (QUE)–isonicotinamide (INM) cocrystal [52] is shown in Figure 2. Structural analysis reveals that the centrosymmetric tetramer assembled by two QUE molecules and two INM molecules is the basic unit of this cocrystal. First, two quercetin molecules form a dimeric unit via the  $R_2^2(10)$  supramolecular homosynthon by means of O–H $\cdots$ O hydrogen bonding interactions (O5–H9 $\cdots$ O6, 2.01 Å, 150°). Subsequently, the QUE homodimeric units are further linked with two INM molecules via N2–H15 $\cdots$ O5 (2.15 Å, 171°) and O6–H10 $\cdots$ O8 (1.78 Å, 172°) hydrogen bonds to form a tetramer. Finally, the tetrameric motif is extended to form a two-dimensional (2D) network through O1–H1 $\cdots$ N1 (1.86 Å, 167°) and N2–H16 $\cdots$ O3 (2.17 Å, 178°) hydrogen bonds. Likewise, tetramers consisting of two drug molecules and two cofomer molecules are also commonly found in the structures of other flavonoid cocrystals, such as fisetin–nicotinamide [63], fisetin–isonicotinamide [66] and luteolin–isonicotinamide [66] cocrystals. In fact, all reported flavonoid cocrystal tetramers have been assembled in the similar pattern so far. In these assemblies, the  $R_2^2(10)$  “homo-dimer” formed by two flavonoid molecules is further linked by nicotinamide or isonicotinamide molecules to form the  $R_3^3(8)$  graph set. This unique tetrameric motif may depend on the common structural features of these flavonoids. For example, in the structures of fisetin, luteolin and quercetin, the two phenolic groups located at the 3'- and 4'-positions of the ortho-position of the benzene ring have the smallest steric hindrance and are more likely to interact with other flavonoid molecules to form dimers.

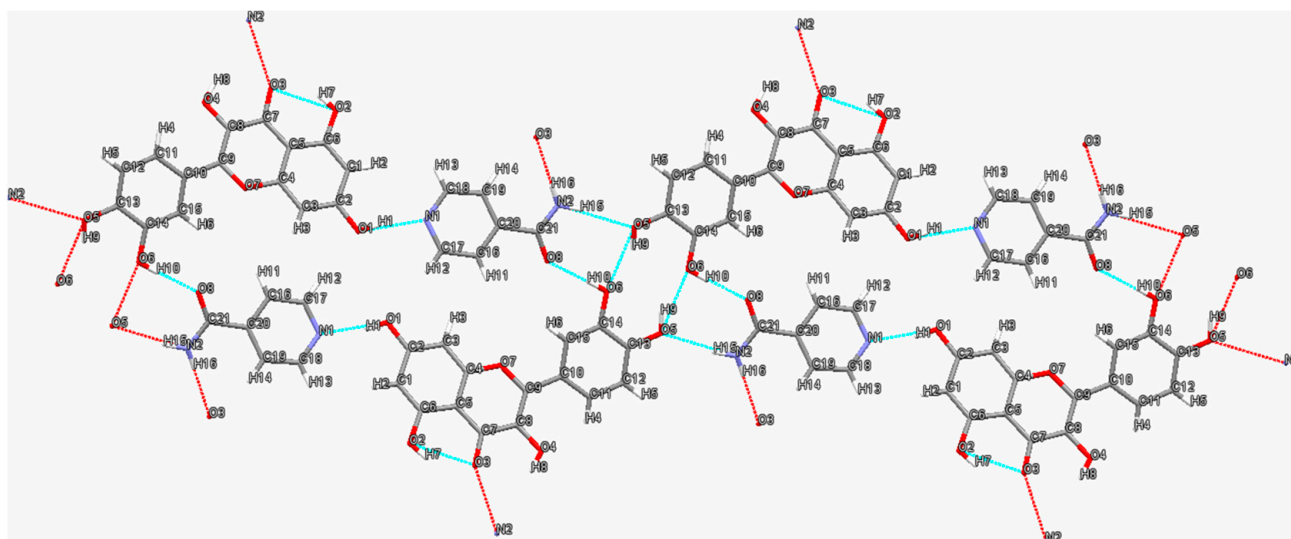


**Figure 2.** Two-dimensional hydrogen bonding network in quercetin–isonicotinamide cocrystal. Hydrogen bonds are indicated by blue dashed lines. Red dashed lines indicate further interactions with other molecules not shown.

### 3.2. Quercetin–Isonicotinic Acid Monohydrate

The two-dimensional hydrogen bonding network in quercetin (QUE)-isonicotinic acid (INA) monohydrate [57] is shown in Figure 3. Apparently, the carboxylate moieties of INA are H-bonded to the hydroxyl moieties on either side of the chains O7–H14...O2 (1.98 Å, 147°) and O3–H10...O4 (1.81 Å, 171°) of the QUE molecules, while the water molecules connect adjacent quercetin molecules via O10–H17...O7 (1.83 Å, 173°) and O5–H11...O10 (1.80 Å, 170°) hydrogen bonds (another quercetin molecule not shown in the figure). The crystal structure of the 1:1 cocrystal monohydrate of QUE and INA contains INA zwitterions that form parallel chains through a N1–H15...O2 (1.57 Å, 170.2°) hydrogen bond, which is supported by the C–N–C angle of 121.7° and C–O bond distances of 1.244 Å and 1.263 Å.

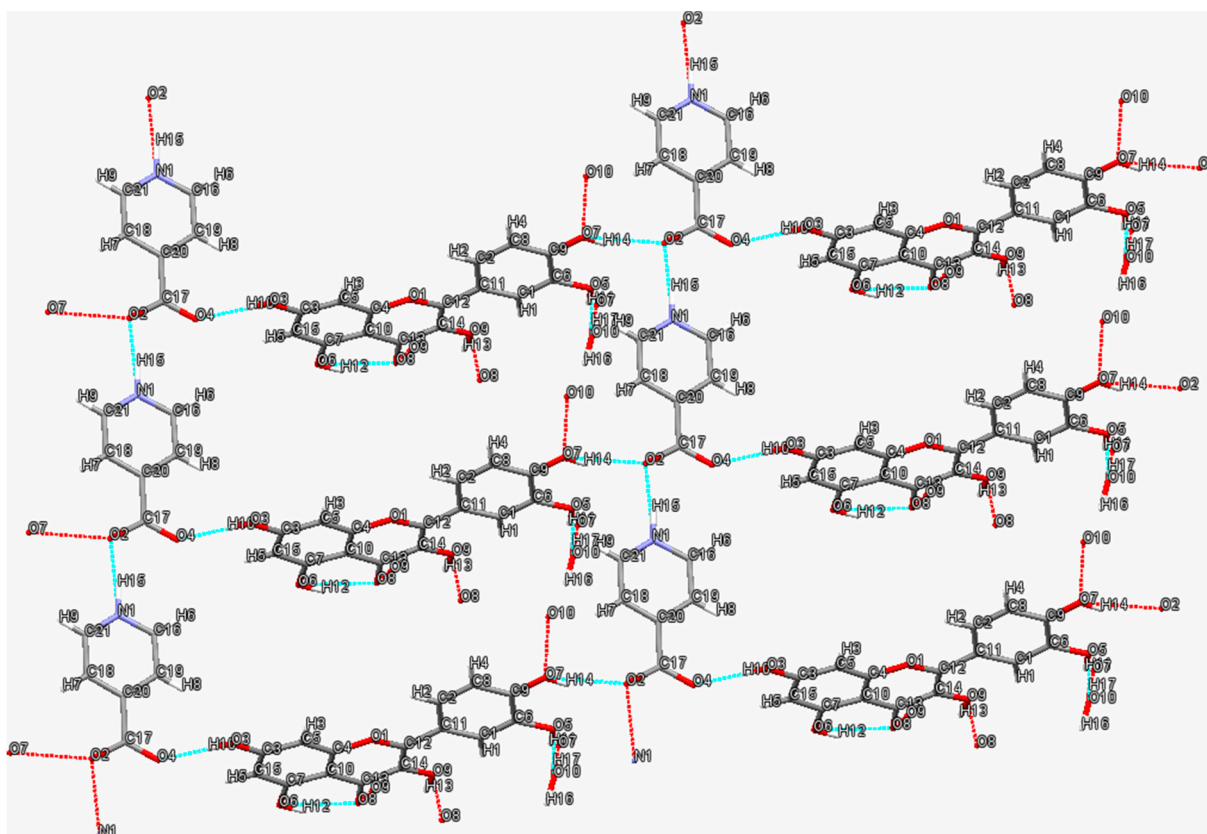


**Figure 3.** Two-dimensional hydrogen bonding network in quercetin-isonicotinic acid monohydrate. Hydrogen bonds are represented by blue dashed lines. Red dashed lines indicate further interactions with other molecules not shown.

### 3.3. Baicalein–Nicotinamide Cocrystal

The two-dimensional hydrogen bond network in the baicalein–nicotinamide cocrystal [68] is shown in Figure 4. Nicotinamide molecules form two types of parallel molecular chains in converse ordinations through N2–H12...O6 (2.23 Å, 145°) hydrogen bonds, and their amide moieties interact with the ortho-phenyl groups of adjacent baicalein molecules via O5–H3...O6 (1.94 Å, 154°) and N2–H11...O4 (2.33 Å, 121°) hydrogen bonds to form heterodimers, while their pyridine nitrogen atoms interact with the neighboring baicalein molecules in the other direction through O4–H2...N1 (1.91 Å, 155°) hydrogen bonds. Every baicalein molecule is connected with two nicotinamide molecules in different chains via O5–H3...O6 (1.94 Å, 154°), N2–H11...O4 (2.33 Å, 121°) and O4–H2...N1 (1.91 Å, 155°) hydrogen bonds, thus forming a tetramer consisting of two baicalein molecules and two nicotinamide molecules. The tetramer extends along the direction parallel to nicotinamide chains to form the hydrogen-bonded networks.

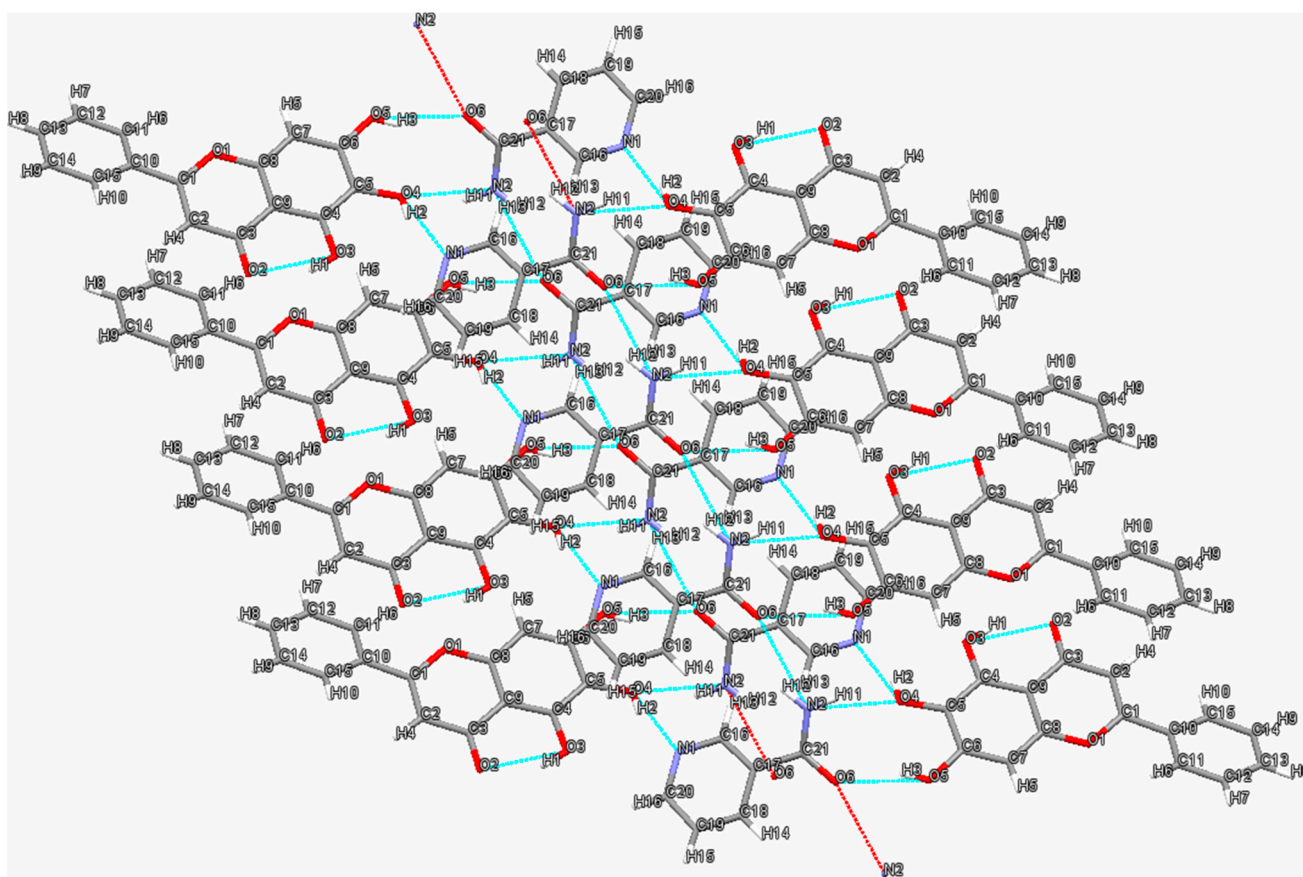


**Figure 4.** Two-dimensional hydrogen bonding network in baicalein-nicotinamide cocrystal. Hydrogen bonds are represented by blue dashed lines. Red dashed lines indicate further interactions with other molecules not shown.

### 3.4. Isoliquiritigenin–Isonicotinamide Cocrystal

The two-dimensional hydrogen bond network of the isoliquiritigenin–isonicotinamide (ISL-INM) cocrystal [78] is displayed in Figure 5. Obviously, ISL and INM molecules are assembled into a sheet structure in their cocrystal. The amide moiety of two adjacent INM molecules is connected by two  $N2-H2A \cdots O5$  (2.03 Å, 172°) hydrogen bonds to form an  $R_2^2(8)$  homodimer, which is connected to the neighboring ISL molecules through the  $O1-H1 \cdots N1$  (1.89 Å, 162°) hydrogen bond. The central INM dimer is capped by a flavonoid molecule at each end, forming a 0-D motif. Then, the 0-D motifs interact with each other through  $N2-H2B \cdots O2$  (2.25 Å, 168°) and  $C14-H14 \cdots O1$  (2.56 Å, 156°) hydrogen bonds to form a 2D sheet structure. Meanwhile, the oxygen atoms (O4) of phenol groups on the adjacent ISL molecules face each other in a close-packed arrangement, which helps to arrange 0-D motifs into a line [80]. Different from other packing types (such as serrated layer), the molecules in the ISL-INM cocrystal are packed into flat layers with relatively large spacing. Under the influence of shear stress, it is easier to slide between neighboring layers, which may lead to higher plasticity and better tableting performance [15,81].

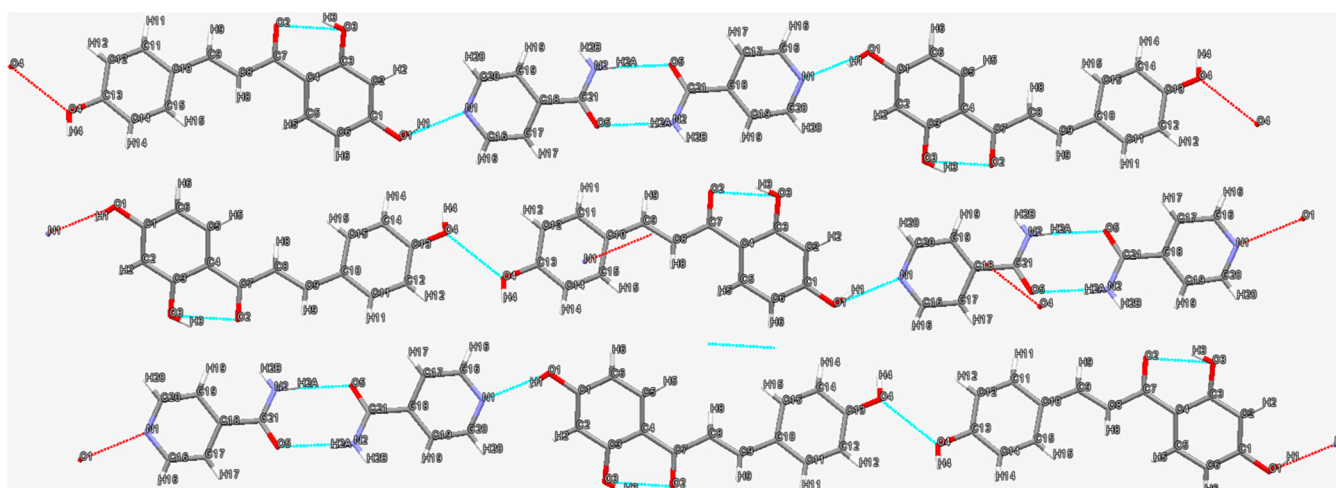


**Figure 5.** Two-dimensional hydrogen bonding network in isoliquiritigenin–isonicotinamide cocrystal. Hydrogen bonds are represented by blue dashed lines. Red dashed lines indicate further interactions with other molecules not shown.

#### 4. Functions of Flavonoid Cocrystals

##### 4.1. Improving Solubility and Bioavailability

Flavonoids are a large family of natural products with a variety of biological activities, including anticancer, anti-inflammatory, antiviral, antioxidant, antibacterial and neuroprotective activities [37–47]. However, the solubility and bioavailability of most flavonoids are poor, which largely limits the further exploitation of flavonoids as drugs [82]. The cocrystallization of flavonoids and soluble cofomers may solve these problems, and several cases are discussed in detail below.

As one of the most abundant flavonoids in the plant kingdom, quercetin (QUE) has numerous therapeutic bioactivities *in vitro* such as antioxidant, metal chelating, antiviral, bacteriostatic, anticarcinogenic and cardioprotective activities [83–88]. However, due to its low solubility and poor bioavailability, its pure form has limited efficacy *in vivo* [89–94]. Smith et al. [52] studied the solubility and bioavailability of four cocrystals formed by quercetin and three different cofomers, including isonicotinamide, theobromine and caffeine. The dissolution curves of four cocrystals (quercetin–isonicotinamide (QUE-INM), quercetin–theobromine dehydrate (QUE-TBR·2H<sub>2</sub>O), quercetin–caffeine (QUE-CAF) and quercetin–caffeine monomethanolate (QUE-CAF·MeOH)) and QUE dihydrate in 50% methanol–water (*v/v*) are shown in Figure 6. It is not difficult to find that each of these cocrystals exhibit superior solubility to quercetin dihydrate. For example, the solubility of QUE dihydrate was 0.267 mg/mL, while the maximum solubilities of quercetin–caffeine, quercetin–caffeine monomethanolate, quercetin–isonicotinamide and quercetin–theobromine dehydrate were 3.627, 2.018, 1.22 and 0.326 mg/mL, respectively. Among these cocrystals, the concentration of quercetin dihydrate in the quercetin–caffeine cocrystal is the highest, and its solubility has increased about 13 times. It is hypothesized that an improvement in the solubility of quercetin will translate into the enhancement of its pharmacokinetic behavior, and the experimental results are shown in Figure 7. As expected, these cocrystals increased the absorption of quercetin in rats by up to 10 times in comparison to quercetin dihydrate.

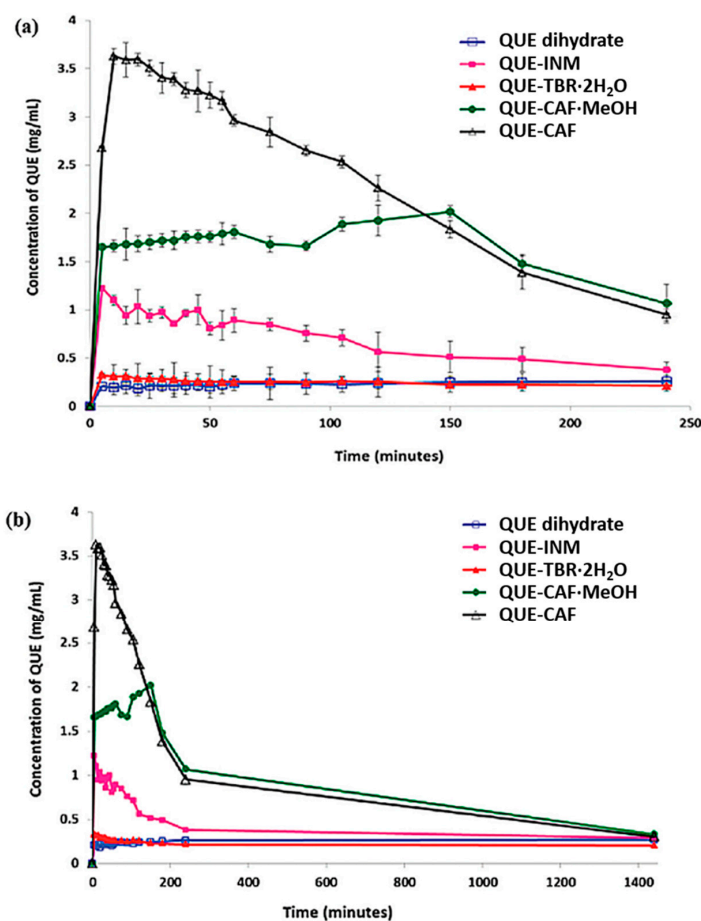


**Figure 6.** Dissolution profiles of QUE dihydrate and QUE cocrystals in 1:1 methanol/water mixture during (a) the first 4 h and (b) 24 h. Adapted from [52] with permission. Copyright © 2011 American Chemical Society.

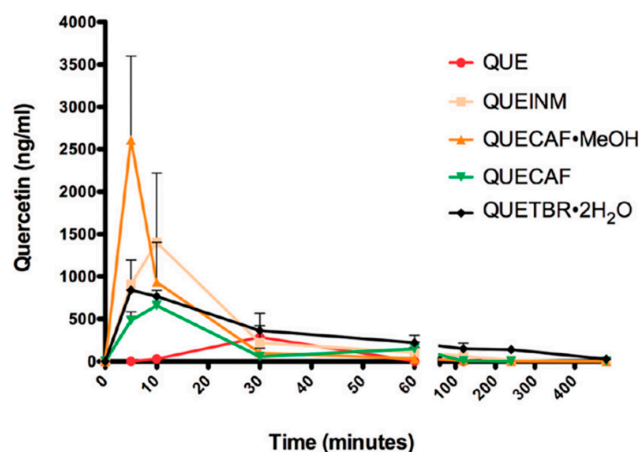


**Figure 7.** Pharmacokinetic profiles of QUE preparations (mean plasma concentration + SD,  $n = 3$ ). Statistical significances were achieved between QUE-INM and QUE at  $t = 10$  min ( $p < 0.01$ ) and between QUE-CAF·MeOH and QUE at  $t = 5$  min ( $p < 0.001$ ), respectively. Adapted from [52] with permission. Copyright © 2011 American Chemical Society.

As an important bioactive flavonoid compound isolated from the root of *Scutellaria baicalensis*, baicalein (Bai) has anti-inflammatory, anticancer, anti-HIV, anti-adipogenic and antibacterial activities [95–101]. Not only that, but it is also included in the *Chinese Pharmacopoeia* as a medication for treating fever, upper respiratory tract infection and sore

throat [102]. However, the application of baicalein in the pharmaceutical field is limited, largely owing to its poor water solubility and low bioavailability [103,104]. Cocrystallization may be an effective way to address the above problems. Zhu et al., reported that baicalein–nicotinamide (BaiNam) cocrystals increased the solubility of baicalein by 50–100% in the pH range of 3.6 to 6.8. In addition, a much larger apparent solubility was also shown in baicalein–caffeine (BaiCaf) and baicalein–isonicotinamide (BaiInam) cocrystals (Figure 8) [69]. In the buffer solutions of pH 2.0 and pH 4.5, the baicalein–caffeine cocrystal resulted in the most significant solubility improvement, which was about 2.5-fold and 1.5-fold that of pure baicalin, respectively [67]. Meanwhile, the maximum solubility of the baicalein–isonicotinamide cocrystal is similar to that of the baicalin–caffeine cocrystal. As the increase in drug solubility may improve its bioavailability, Zhu et al. studied the bioavailability of the baicalein–caffeine cocrystal, a baicalein–caffeine physical mixture and pure baicalin in rats to confirm this [69]. Since baicalein-7-O-glucuronide (BG) is the main active metabolite of Bai and the mainly existing form in plasma, BG was provided for statistical comparison and bioavailability calculation. As shown in Figure 9, The  $C_{max}$  and  $AUC_{0-24h}$  of the baicalein–caffeine cocrystal were 2.35-fold and 4.14-fold higher than those of pure baicalin (Bai), respectively, which were also significantly higher than those of their physical mixture (PM).

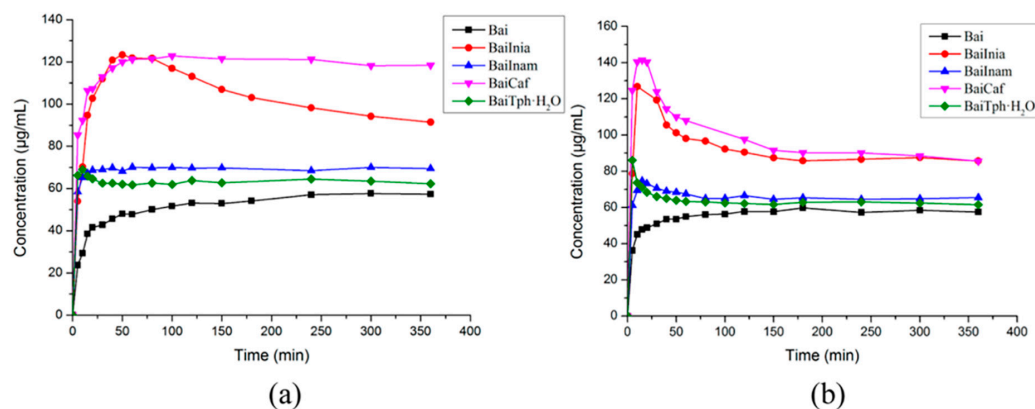


**Figure 8.** Powder dissolution profiles of Bai and its four cocrystals (BaiInia (baicalein–isoniazide), BaiInam (baicalein–isonicotinamide), BaiCaf (baicalein–caffeine) and BaiTph·H<sub>2</sub>O (baicalein–theophylline monohydrate)) in (a) pH 2.0 and (b) pH 4.5 buffer solutions. Adapted from [69] with permission. Copyright © 2017 American Chemical Society.

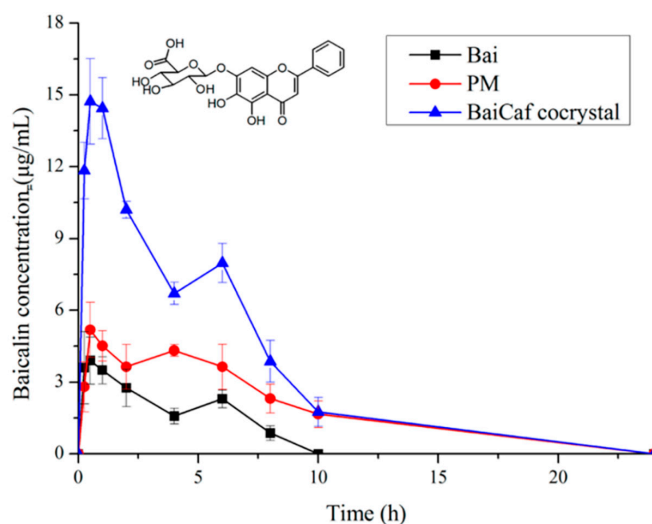


**Figure 9.** Plasma BG concentration–time curves of the crystalline Bai, PM and BaiCaf cocrystal (data are expressed as means  $\pm$  SD,  $n = 6$ ). Adapted from [69] with permission. Copyright © 2017 American Chemical Society.

In addition, kaempferol with tetrahydroxyflavone structure is one of the most common aglycone flavonoids, which exists in various parts of plants in the form of glycosides, including seeds, leaves, fruits, flowers and even vegetables. It has been proven that kaempferol and its glycosylated derivatives have a variety of pharmacological activities, such as osteoprotective, anticancer, neuroprotective, anti-inflammatory, antidiabetic, antioxidant, antimicrobial, chemo-preventive and therapeutic activities [105–111]. However, like other flavonoids mentioned above, the solubility of kaempferol in water is very low, which leads to poor absorption in vivo [94,112,113]. Recently, a kaempferol-L-proline cocrystal was synthesized, and its solubility and bioavailability are higher than those of pure kaempferol [58]. The dissolution experiment of the powders in a 0.5% Tween 80 system showed that the maximum solubility of the kaempferol-L-proline cocrystal was about 270% higher than that of pure kaempferol. Meanwhile, the pharmacokinetic curves of kaempferol (Kae), the kaempferol-L-proline (Kae-L-Pro) cocrystal, and a physical mixture (PM) of kaempferol and L-proline are presented in Figure 10. As the main metabolite of Kae in blood, the pharmacokinetic parameters of Kae-3-O-glucoside were provided and analyzed. The results showed that the pharmacokinetic curve of the Kae-L-Pro cocrystal was improved compared with the pure Kae component and corresponding physical mixture, and its  $C_{max}$  and  $AUC_{0-24h}$  were 369% and 351% higher than those of the pure Kae, respectively.

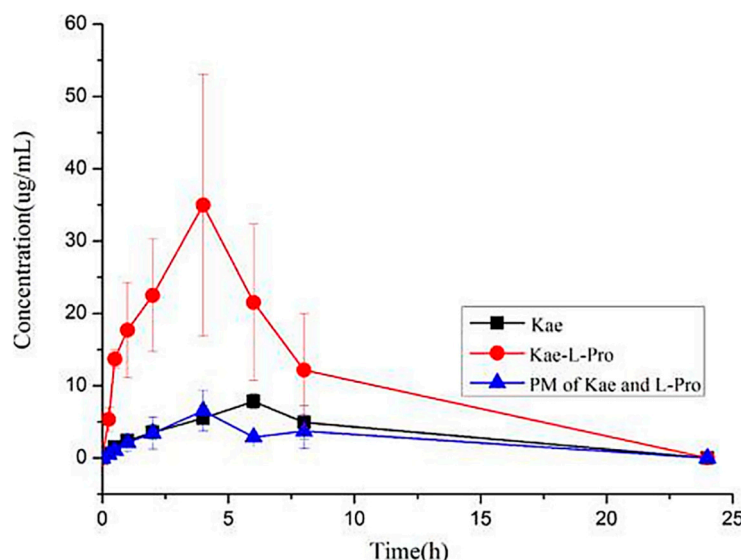


**Figure 10.** Pharmacokinetic profiles of Kae-3-O-glucoside after administration of kaempferol (Kae), kaempferol-L-proline (Kae-L-Pro) and physical mixture (PM) of Kae and L-Pro (mean plasma concentration versus time). Data are expressed as means  $\pm$  SD,  $n = 6$ . Adapted from [58] with permission. Copyright © 2016 American Chemical Society.

Chrysin, isolated from various plants such as the blue passion flower (*Passiflora caerulea* L.), is a flavonoid compound with a variety of pharmacological activities including antidiabetic, anti-inflammatory, and antitumor activities [114–116]. Sa et al., reported a novel salt cocrystal of chrysin (ChrH) and berberine (BerbOH) [71], which is also a new drug–drug cocrystal based on two natural products. An in vivo bioavailability study on pure chrysin and chrysin in the form of the cocrystal was performed, and the mean plasma concentrations of chrysin in the two forms versus time profiles are shown in Figure 11. The results show that the chrysin cocrystal has higher  $C_{max}$  and AUC than pure chrysin. According to the  $AUC_{0-24h}$  results, the relative bioavailability of the chrysin cocrystal is about 1.7 times of that of pure chrysin. Although the improvement of  $C_{max}$  and AUC is modest, this work provides a new strategy for the design of drug–drug cocrystals based on alkaloids and flavonoids through charge-assisted strong hydrogen bonding interactions.

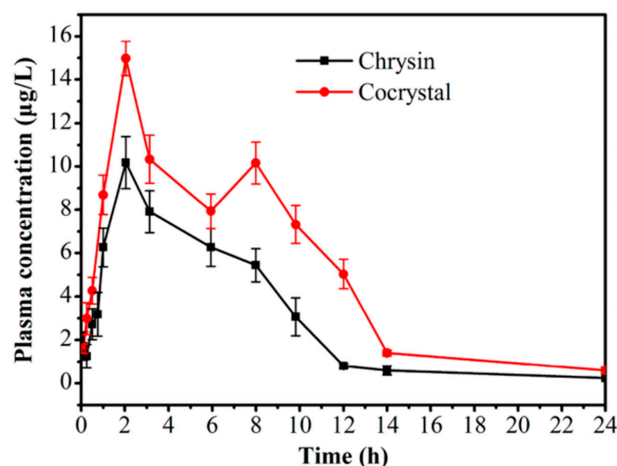


**Figure 11.** Mean plasma concentrations versus time profiles of chrysin and cocrystal. Adapted from [71] with permission. Copyright © 2018 American Chemical Society.

#### 4.2. Optimizing Other Properties

The cocrystallization of flavonoids can not only improve the solubility and bioavailability of APIs, but also adjust many other properties such as pharmacodynamic properties, photoluminescent properties, etc.

##### 4.2.1. Improving Pharmacodynamic Response

Hesperetin, commonly found in citrus fruits, is a powerful antioxidant molecule and belongs to dihydroflavonoids. It also exhibits antiplatelet, anti-inflammatory, antiviral and antibacterial effects, as well as prominent protective effects on carcinoid, lung, breast and colon cancers [117–124]. In order to evaluate the pharmacodynamic differences between hesperidin and its cocrystals, Kunal et al. studied their anti-inflammatory activity [72], and the percent inhibitions of inflammation of hesperetin (HESP), the hesperetin–picolinic acid cocrystal (HESP-PICO), the hesperetin–nicotinamide cocrystal (HESP-NICO) and the hesperetin–caffeine cocrystal (HESP-CAFF) are shown in Figure 12. Obviously, the inflammation inhibitory effect of pure hesperetin was weaker than its cocrystals at all time points, and all three cocrystals exhibited improved anti-inflammatory activity. After 240 min of carrageenan injection, all compounds generally reached the maximum inflammation inhibition percentage. At this moment, compared with the anti-inflammatory inhibition rate of 60% of pure hesperetin, HESP-CAFF showed the strongest anti-inflammatory activity, with an inflammation inhibition rate of 87%, while HESP-NICO and HESP-PICO also showed better anti-inflammatory activity, with inhibition rates of 79% and 72%, respectively. These impressive data indicate that cocrystals have a clear advantage over the drug itself in achieving the desired pharmacological response.

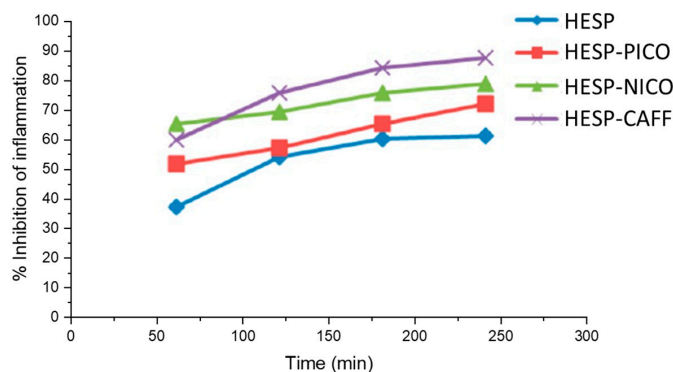


**Figure 12.** Percent inhibition of inflammation of HESP, HESP-PICO, HESP-NICO and HESP-CAFF. Adapted from [72] with permission. Copyright © 2017 American Chemical Society.

In addition, Kunal et al. also studied the antioxidant and antihemolytic activities of hesperetin cocrystals [72]. As shown in Figure 13, compared with pure hesperidin, the antioxidant activity of hesperetin cocrystals measured by the oxidation inhibition percentage of the 1,1-diphenyl-2-picryl hydroxyl (DPPH) free radical increased, indicating that the activity of HESP-CAFF increased by nearly 50%, the activity of HESP-NICO increased by about 30% and the activity of HESP-PICO increased by 20%. Figure 14 lucidly depicts that compared with the cocrystals, hesperidin has a much lower inhibitory effect on the hemolysis of rat red blood cells (RBCs). On the average of all tested concentrations, the hemolysis rate of rat RBCs was significantly reduced, with a maximum 60% decrease by HESP-CAFF, followed by a nearly 40% decrease by HESP-NICO and about 30% by HESP-PICO, over that of pure hesperidin.

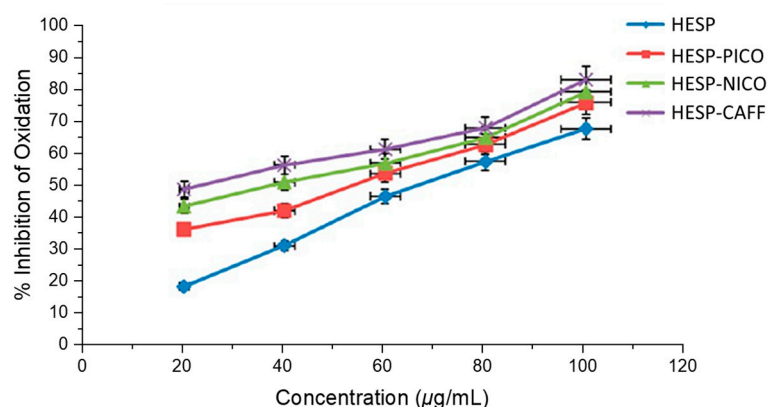


**Figure 13.** Percentage inhibition of oxidation of DPPH radical by hesperidin and the cocrystals. Adapted from [72] with permission. Copyright © 2017 American Chemical Society.

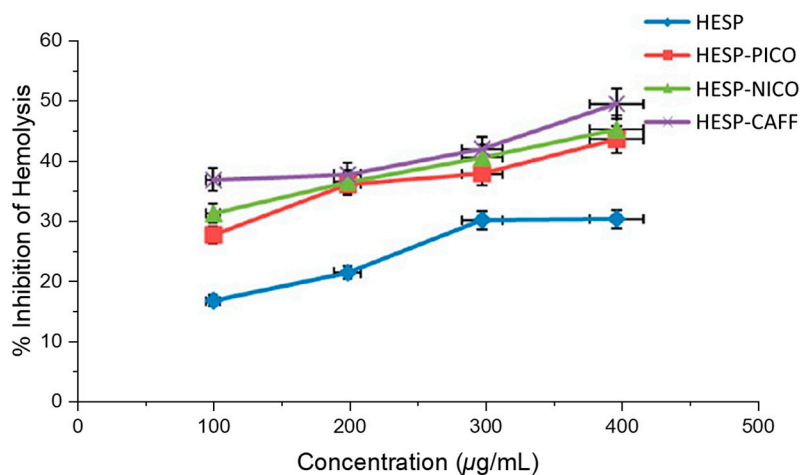


**Figure 14.** Antihemolytic activity represented as the percentage inhibition of hemolysis by hesperidin and the cocrystals. Adapted from [72] with permission. Copyright © 2017 American Chemical Society.

#### 4.2.2. Tuning Photoluminescent Properties

Phloretin (PHL), extracted from the pericarp and velamen of apples or pears, is a dihydrochalcone flavonoid. It not only has many pharmacological activities including antioxidant, anticancer and anti-inflammatory effects, but also can suppress the growth, virulence and biofilm formation of Gram-negative and Gram-positive bacteria [125–132]. Recently, in order to improve the solubility of phloretin, Huang et al. synthesized phloretin-nicotinamide (PHL-NIC) and phloretin-isonicotinamide (PHL-INM) cocrystals, and observed that phloretin, the PHL-NIC cocrystal and the PHL-INM cocrystal have apparently different photoluminescent properties [79]. As shown in Figure 15, under a 365 nm UV lamp, the PHL-NIC cocrystal exhibited strong yellowish-green fluorescence, while PHL

and the PHL-INM cocrystal showed almost no fluorescence under the same condition. This result indicates that the introduction of the NIC cofomer can significantly affect the photoluminescent properties of phloretin, while the introduction of the INM cofomer cannot. The different photoluminescence properties of these two cocrystals may be attributed to the varied intermolecular interactions and stacking arrangements in their structures. From the perspective of cocrystal structure, compared to the sheet (planar) structure of the PHL-INM cocrystal with a shorter ring centroid–centroid (Cg-Cg) distance, the zigzag packing of the PHL-NIC cocrystal with a longer ring centroid–centroid (Cg-Cg) distance may enhance the emission of the PHL-NIC cocrystal in the solid state, resulting in high luminescent property. Additionally, the Hirshfeld surface analysis results of PHL molecules on PHL-NIC and PHL-INM cocrystals also quantitatively support this conclusion. The  $\pi$ - $\pi$  interaction of the PHL-NIC cocrystal is 10.5%, which is lower than that of the PHL-INM cocrystal (12.5%). These results imply that the photoluminescence properties of flavonoid cocrystals can be tuned by the introduction of cofomers.

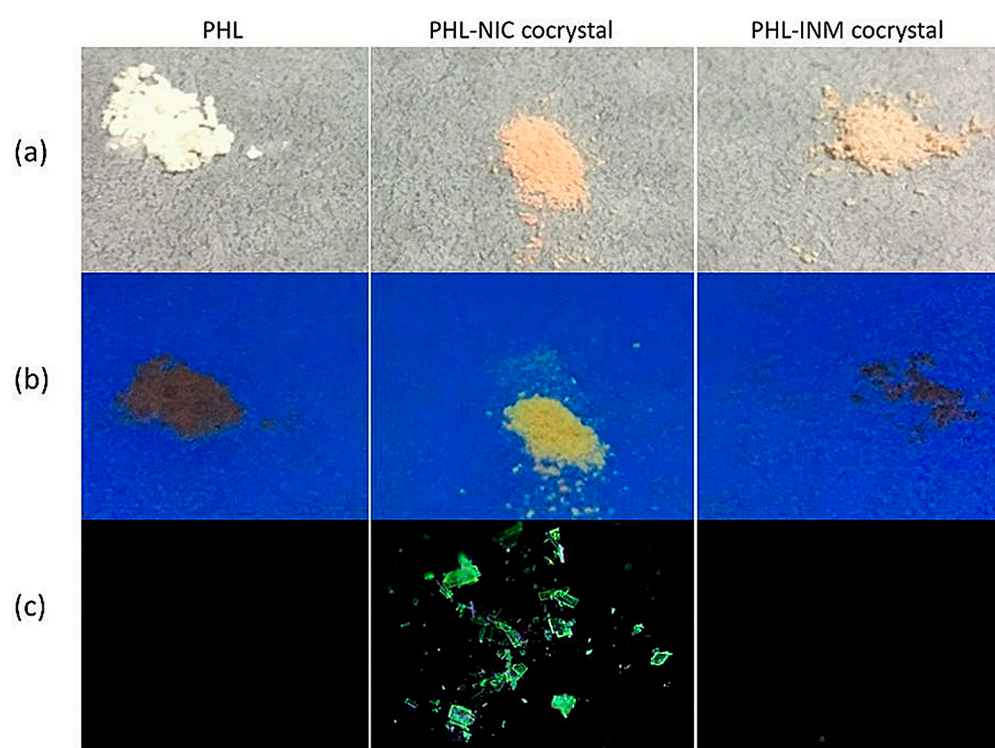


**Figure 15.** Photographs of solid-state cocrystal samples (from left to right: PHL, PHL-NIC cocrystal and PHL-INM cocrystal): (a) the powder samples under daylight; (b) the powder samples under UV (365 nm) lamp; (c) the single crystal samples under UV (365 nm) observed by polarized microscope. Adapted from [79] with permission. Copyright © 2019 American Chemical Society.

## 5. Conclusions

Pharmaceutical cocrystals are currently a rapidly developing field, because they can favorably alter the physicochemical properties of APIs. Recently, benefiting from the polyphenolic structure, cocrystallization has become an effective method in improving the properties of flavonoids. In this review, we summarized the cocrystals synthesized from different flavonoids and cofomers and discussed in detail that phenolic groups tend to form intermolecular hydrogen bonds with the cofomers. On this basis, we presumed that flavonoids with a phenolic group at the 7-position or 4'-position are more likely to form cocrystals and discussed the different intermolecular and intramolecular interactions in their solid forms by analyzing the crystal structures of some typical flavonoid cocrystals. The tetramer composed of two flavonoid molecules and two nicotinamide or isonicotinamide molecules, which exists in the crystal structures of quercetin–isonicotinamide and

fisetin–nicotinamide cocrystals, is the most typical arrangement. In most cases, the purpose of synthesizing flavonoid cocrystals is to improve solubility and bioavailability. Therefore, it is preferable to select the cofomers with high solubility (e.g., nicotinamide and isonicotinamide) in the GRAS list. In addition, the cocrystallization of flavonoids may also alter other properties. Flavonoid cocrystals have a good prospect in clinical translation, and the analysis of possible hydrogen bond sites and hydrogen bond networks in this review is helpful for the targeted synthesis of flavonoid cocrystals.

**Author Contributions:** J.X. (Jia Xu): Writing—original draft preparation; Q.S.: Writing—review and editing; Y.W. (Yanan Wang): Writing—part 1; Y.W. (Yong Wang): Writing—part 2; J.X. (Junbo Xin): Writing—part 3; J.C.: Writing—part 4; F.L.: Writing—review and editing. All authors have read and agreed to the published version of the manuscript.

**Funding:** This research was funded by the Natural Science Foundation of Jiangsu Province (No. BK20211114), Natural Science Foundation of the College of Jiangsu Province (No. 21KJB350016), the “Qing-Lan” Project of Jiangsu Colleges and the Research Startup Fund of Jiangsu Vocational College of Medicine (No. 20216104, No. 20200018).

**Institutional Review Board Statement:** Not applicable.

**Informed Consent Statement:** Not applicable.

**Data Availability Statement:** Not applicable.

**Conflicts of Interest:** The authors declare that they have no conflict of interest.

## References

1. Karimi-Jafari, M.; Padrela, L.; Walker, G.M.; Croker, D.M. Creating Cocrystals: A Review of Pharmaceutical Cocrystal Preparation Routes and Applications. *Cryst. Growth Des.* **2018**, *18*, 6370–6387. [[CrossRef](#)]
2. Kavanagh, O.N.; Croker, D.M.; Walker, G.M.; Zaworotko, M.J. Pharmaceutical cocrystals: From serendipity to design to application. *Drug Discov. Today* **2019**, *24*, 796–804. [[CrossRef](#)] [[PubMed](#)]
3. Healy, A.M.; Worku, Z.A.; Kumar, D.; Madi, A.M. Pharmaceutical solvates, hydrates and amorphous forms: A special emphasis on cocrystals. *Adv. Drug Deliv. Rev.* **2017**, *117*, 25–46. [[CrossRef](#)] [[PubMed](#)]
4. Chen, J.; Sarma, B.; Evans, J.M.B.; Myerson, A.S. Pharmaceutical Crystallization. *Cryst. Growth Des.* **2011**, *11*, 887–895. [[CrossRef](#)]
5. Ter Horst, J.H.; Deij, M.A.; Cains, P.W. Discovering New Co-Crystals. *Cryst. Growth Des.* **2009**, *9*, 1531–1537. [[CrossRef](#)]
6. Guo, M.; Sun, X.; Chen, J.; Cai, T. Pharmaceutical cocrystals: A review of preparations, physicochemical properties and applications. *Acta Pharm. Sin. B* **2021**, *11*, 2537–2564. [[CrossRef](#)]
7. Berry, D.J.; Steed, J.W. Pharmaceutical cocrystals, salts and multicomponent systems; intermolecular interactions and property based design. *Adv. Drug Deliv. Rev.* **2017**, *117*, 3–24. [[CrossRef](#)]
8. Shan, N.; Zaworotko, M.J. The role of cocrystals in pharmaceutical science. *Drug Discov. Today* **2008**, *13*, 440–446. [[CrossRef](#)]
9. Thakuria, R.; Delori, A.; Jones, W.; Lipert, M.P.; Roy, L.; Rodríguez-Hornedo, N. Pharmaceutical cocrystals and poorly soluble drugs. *Int. J. Pharm.* **2013**, *453*, 101–125. [[CrossRef](#)]
10. Sun, C.C. Cocrystallization for successful drug delivery. *Expert Opin. Drug Deliv.* **2013**, *10*, 201–213. [[CrossRef](#)]
11. Chen, Y.; Li, L.; Yao, J.; Ma, Y.-Y.; Chen, J.-M.; Lu, T.-B. Improving the Solubility and Bioavailability of Apixaban via Apixaban–Oxalic Acid Cocrystal. *Cryst. Growth Des.* **2016**, *16*, 2923–2930. [[CrossRef](#)]
12. Childs, S.L.; Chyall, L.J.; Dunlap, J.T.; Smolenskaya, V.N.; Stahly, B.C.; Stahly, G.P. Crystal Engineering Approach To Forming Cocrystals of Amine Hydrochlorides with Organic Acids. Molecular Complexes of Fluoxetine Hydrochloride with Benzoic, Succinic, and Fumaric Acids. *J. Am. Chem. Soc.* **2004**, *126*, 13335–13342. [[CrossRef](#)]
13. Vangala, V.R.; Chow, P.S.; Tan, R.B.H. Characterization, physicochemical and photo-stability of a co-crystal involving an antibiotic drug, nitrofurantoin, and 4-hydroxybenzoic acid. *CrystEngComm* **2011**, *13*, 759–762. [[CrossRef](#)]
14. Gao, Y.; Zu, H.; Zhang, J. Enhanced dissolution and stability of adefovir dipivoxil by cocrystal formation. *J. Pharm. Pharmacol.* **2011**, *63*, 483–490. [[CrossRef](#)]
15. Chow, S.F.; Chen, M.; Shi, L.; Chow, A.H.L.; Sun, C.C. Simultaneously Improving the Mechanical Properties, Dissolution Performance, and Hygroscopicity of Ibuprofen and Flurbiprofen by Cocrystallization with Nicotinamide. *Pharm. Res.* **2012**, *29*, 1854–1865. [[CrossRef](#)]
16. Karki, S.; Friščić, T.; Fábrián, L.; Laity, P.R.; Day, G.M.; Jones, W. Improving Mechanical Properties of Crystalline Solids by Cocrystal Formation: New Compressible Forms of Paracetamol. *Adv. Mater.* **2009**, *21*, 3905–3909. [[CrossRef](#)]
17. Sun, C.C.; Hou, H. Improving Mechanical Properties of Caffeine and Methyl Gallate Crystals by Cocrystallization. *Cryst. Growth Des.* **2008**, *8*, 1575–1579. [[CrossRef](#)]
18. Jermain, S.V.; Brough, C.; Williams, R.O. Amorphous solid dispersions and nanocrystal technologies for poorly water-soluble drug delivery—An update. *Int. J. Pharm.* **2018**, *535*, 379–392. [[CrossRef](#)]

19. Thakuria, R.; Nangia, A. Olanzapinium Salts, Isostructural Solvates, and Their Physicochemical Properties. *Cryst. Growth Des.* **2013**, *13*, 3672–3680. [[CrossRef](#)]
20. Aitipamula, S.; Banerjee, R.; Bansal, A.K.; Biradha, K.; Cheney, M.L.; Choudhury, A.R.; Desiraju, G.R.; Dikundwar, A.G.; Dubey, R.; Duggirala, N.; et al. Polymorphs, Salts, and Cocrystals: What's in a Name? *Cryst. Growth Des.* **2012**, *12*, 2147–2152. [[CrossRef](#)]
21. Bernstein, J. Polymorphism—A Perspective. *Cryst. Growth Des.* **2011**, *11*, 632–650. [[CrossRef](#)]
22. Pudipeddi, M.; Serajuddin, A.T. Trends in solubility of polymorphs. *J. Pharm. Sci.* **2005**, *94*, 929–939. [[CrossRef](#)] [[PubMed](#)]
23. Ciumarnean, L.; Milaciu, M.V.; Runcan, O.; Vesa, S.C.; Rachisan, A.L.; Negrean, V.; Perne, M.G.; Donca, V.I.; Alexescu, T.G.; Para, I.; et al. The Effects of Flavonoids in Cardiovascular Diseases. *Molecules* **2020**, *25*, 4320. [[CrossRef](#)] [[PubMed](#)]
24. Zeng, X.; Xi, Y.; Jiang, W. Protective roles of flavonoids and flavonoid-rich plant extracts against urolithiasis: A review. *Crit. Rev. Food Sci. Nutr.* **2019**, *59*, 2125–2135. [[CrossRef](#)] [[PubMed](#)]
25. Perez-Vizcaino, F.; Fraga, C.G. Research trends in flavonoids and health. *Arch. Biochem. Biophys.* **2018**, *646*, 107–112. [[CrossRef](#)]
26. Zakaryan, H.; Arabyan, E.; Oo, A.; Zandi, K. Flavonoids: Promising natural compounds against viral infections. *Arch. Virol.* **2017**, *162*, 2539–2551. [[CrossRef](#)]
27. Fernandes, I.; Perez-Gregorio, R.; Soares, S.; Mateus, N.; de Freitas, V. Wine Flavonoids in Health and Disease Prevention. *Molecules* **2017**, *22*, 292. [[CrossRef](#)]
28. Peluso, I.; Miglio, C.; Morabito, G.; Ioannone, F.; Serafini, M. Flavonoids and immune function in human: A systematic review. *Crit. Rev. Food Sci. Nutr.* **2015**, *55*, 383–395. [[CrossRef](#)]
29. Serafini, M.; Peluso, I.; Raguzzini, A. Flavonoids as anti-inflammatory agents. *Proc. Nutr. Soc.* **2010**, *69*, 273–278. [[CrossRef](#)]
30. Cushnie, T.P.; Lamb, A.J. Antimicrobial activity of flavonoids. *Int. J. Antimicrob. Agents* **2005**, *26*, 343–356. [[CrossRef](#)]
31. Ross, J.A.; Kasum, C.M. Dietary flavonoids: Bioavailability, metabolic effects, and safety. *Annu. Rev. Nutr.* **2002**, *22*, 19–34. [[CrossRef](#)]
32. Nijveldt, R.; van Nood, E.; van Hoorn, D.E.; Boelens, P.; van Norren, K.; van Leeuwen, P.A. Flavonoids: A review of probable mechanisms of action and potential applications. *Am. J. Clin. Nutr.* **2001**, *74*, 418–425. [[CrossRef](#)]
33. Kumar, S.; Pandey, A.K. Chemistry and biological activities of flavonoids: An overview. *Sci. World J.* **2013**, *2013*, 162750. [[CrossRef](#)]
34. Kumar, S.; Mishra, A.; Pandey, A.K. Antioxidant mediated protective effect of Parthenium hysterophorus against oxidative damage using in vitro models. *BMC Complement. Altern. Med.* **2013**, *13*, 120. [[CrossRef](#)]
35. Cook, N.C.; Samman, S. Flavonoids—Chemistry, metabolism, cardioprotective effects, and dietary sources. *J. Nutr. Biochem.* **1996**, *7*, 66–76. [[CrossRef](#)]
36. Middleton, E. Effect of plant flavonoids on immune and inflammatory cell function. *Adv. Exp. Med. Biol.* **1998**, *439*, 175–182.
37. Ming, X.; Ding, M.; Zhai, B.; Xiao, L.; Piao, T.; Liu, M. Biochanin A inhibits lipopolysaccharide-induced inflammation in human umbilical vein endothelial cells. *Life Sci.* **2015**, *136*, 36–41. [[CrossRef](#)]
38. Kole, L.; Giri, B.; Manna, S.K.; Pal, B.; Ghosh, S. Biochanin-A, an isoflavon, showed anti-proliferative and anti-inflammatory activities through the inhibition of iNOS expression, p38-MAPK and ATF-2 phosphorylation and blocking NFκB nuclear translocation. *Eur. J. Pharmacol.* **2011**, *653*, 8–15. [[CrossRef](#)]
39. Michaelis, M.; Sithisarn, P.; Cinatl, J., Jr. Effects of flavonoid-induced oxidative stress on anti-H5N1 influenza A virus activity exerted by baicalin and biochanin A. *BMC Res. Notes* **2014**, *7*, 384. [[CrossRef](#)]
40. Puli, S.; Lai, J.C.K.; Bhushan, A. Inhibition of matrix degrading enzymes and invasion in human glioblastoma (U87MG) Cells by isoflavones. *J. Neuro-Oncol.* **2006**, *79*, 135–142. [[CrossRef](#)]
41. Havsteen, B.H. The biochemistry and medical significance of the flavonoids. *Pharmacol. Ther.* **2002**, *96*, 67–202. [[CrossRef](#)] [[PubMed](#)]
42. Harborne, J.B.; Williams, C.A. Advances in flavonoid research since 1992. *Phytochemistry* **2000**, *55*, 481–504. [[CrossRef](#)] [[PubMed](#)]
43. Chin, Y.W.; Jung, H.A.; Liu, Y.; Su, B.N.; Castoro, J.A.; Keller, W.J.; Pereira, M.A.; Kinghorn, A.D. Anti-oxidant constituents of the roots and stolons of licorice (*Glycyrrhiza glabra*). *J. Agric. Food Chem.* **2007**, *55*, 4691–4697. [[CrossRef](#)] [[PubMed](#)]
44. Lee, S.H.; Kim, J.Y.; Seo, G.S.; Kim, Y.C.; Sohn, D.H. Isoliquiritigenin, from *Dalbergia odorifera*, up-regulates anti-inflammatory heme oxygenase-1 expression in RAW264.7 macrophages. *Inflamm. Res.* **2009**, *58*, 257–262. [[CrossRef](#)] [[PubMed](#)]
45. Maggiolini, M.; Statti, G.; Vivacqua, A.; Gabriele, S.; Rago, V.; Loizzo, M.; Menichini, F.; Amdò, S. Estrogenic and antiproliferative activities of isoliquiritigenin in MCF7 breast cancer cells. *J. Steroid Biochem. Mol. Biol.* **2002**, *82*, 315–322. [[CrossRef](#)]
46. Choi, Y.H.; Kim, Y.J.; Chae, H.S.; Chin, Y.W. In vivo gastroprotective effect along with pharmacokinetics, tissue distribution and metabolism of isoliquiritigenin in mice. *Planta Med.* **2015**, *81*, 586–593. [[CrossRef](#)]
47. Kanazawa, M.; Satomi, Y.; Mizutani, Y.; Ukimura, O.; Kawachi, A.; Sakai, T.; Baba, M.; Okuyama, T.; Nishino, H.; Miki, T. Isoliquiritigenin Inhibits the Growth of Prostate Cancer. *Eur. Urol.* **2003**, *43*, 580–586. [[CrossRef](#)]
48. Chebil, L.; Humeau, C.; Anthoni, J. Solubility of Flavonoids in Organic Solvents. *J. Chem. Eng. Data* **2007**, *52*, 1552–1556. [[CrossRef](#)]
49. Timmons, D.J.; Pacheco, M.R.; Fricke, K.A.; Sleboznick, C. Assembling Extended Structures with Flavonoids. *Cryst. Growth Des.* **2008**, *8*, 2765–2769. [[CrossRef](#)]
50. Huang, S.; Xue, Q.; Xu, J.; Ruan, S.; Cai, T. Simultaneously Improving the Physicochemical Properties, Dissolution Performance, and Bioavailability of Apigenin and Daidzein by Co-Crystallization with Theophylline. *J. Pharm. Sci.* **2019**, *108*, 2982–2993. [[CrossRef](#)]

51. Dubey, R.; Desiraju, G.R. Combinatorial selection of molecular conformations and supramolecular synthons in quercetin cocrystal landscapes: A route to ternary solids. *IUCrJ* **2015**, *2*, 402–408. [[CrossRef](#)]
52. Smith, A.J.; Kavuru, P.; Wojtas, L.; Zaworotko, M.J.; Shytle, R.D. Cocrystals of quercetin with improved solubility and oral bioavailability. *Mol. Pharm.* **2011**, *8*, 1867–1876. [[CrossRef](#)]
53. Vasisht, K.; Chadha, K.; Karan, M.; Bhalla, Y.; Jena, A.K.; Chadha, R. Enhancing biopharmaceutical parameters of bioflavonoid quercetin by cocrystallization. *CrystEngComm* **2016**, *18*, 1403–1415. [[CrossRef](#)]
54. Veverka, M.; Dubaj, T.; Gallovič, J.; Jorík, V.; Veverková, E.; Danihelová, M.; Šimon, P. Cocrystals of quercetin: Synthesis, characterization, and screening of biological activity. *Monatsh. Chem.* **2014**, *146*, 99–109. [[CrossRef](#)]
55. Zhang, Y.-N.; Yin, H.-M.; Zhang, Y.; Zhang, D.-J.; Su, X.; Kuang, H.-X. Cocrystals of kaempferol, quercetin and myricetin with 4,4'-bipyridine: Crystal structures, analyses of intermolecular interactions and antibacterial properties. *J. Mol. Struct.* **2017**, *1130*, 199–207. [[CrossRef](#)]
56. Clarke, H.D.; Arora, K.K.; Bass, H.; Kavuru, P.; Ong, T.T.; Pujari, T.; Wojtas, L.; Zaworotko, M.J. Structure–Stability Relationships in Cocrystal Hydrates: Does the Promiscuity of Water Make Crystalline Hydrates the Nemesis of Crystal Engineering? *Cryst. Growth Des.* **2010**, *10*, 2152–2167. [[CrossRef](#)]
57. Kavuru, P.; Aboarayas, D.; Arora, K.K.; Clarke, H.D.; Kennedy, A.; Marshall, L.; Ong, T.T.; Perman, J.; Pujari, T.; Wojtas, L.; et al. Hierarchy of Supramolecular Synthons: Persistent Hydrogen Bonds Between Carboxylates and Weakly Acidic Hydroxyl Moieties in Cocrystals of Zwitterions. *Cryst. Growth Des.* **2010**, *10*, 3568–3584. [[CrossRef](#)]
58. He, H.; Huang, Y.; Zhang, Q.; Wang, J.-R.; Mei, X. Zwitterionic Cocrystals of Flavonoids and Proline: Solid-State Characterization, Pharmaceutical Properties, and Pharmacokinetic Performance. *Cryst. Growth Des.* **2016**, *16*, 2348–2356. [[CrossRef](#)]
59. Liu, F.; Wang, L.-Y.; Li, Y.-T.; Wu, Z.-Y.; Yan, C.-W. Protective Effects of Quercetin against Pyrazinamide Induced Hepatotoxicity via a Cocrystallization Strategy of Complementary Advantages. *Cryst. Growth Des.* **2018**, *18*, 3729–3733. [[CrossRef](#)]
60. Hong, C.; Xie, Y.; Yao, Y.; Li, G.; Yuan, X.; Shen, H. A novel strategy for pharmaceutical cocrystal generation without knowledge of stoichiometric ratio: Myricetin cocrystals and a ternary phase diagram. *Pharm. Res.* **2015**, *32*, 47–60. [[CrossRef](#)]
61. Liu, M.; Hong, C.; Yao, Y.; Shen, H.; Ji, G.; Li, G.; Xie, Y. Development of a pharmaceutical cocrystal with solution crystallization technology: Preparation, characterization, and evaluation of myricetin-proline cocrystals. *Eur. J. Pharm. Biopharm.* **2016**, *107*, 151–159. [[CrossRef](#)]
62. Mureşan-Pop, M.; Chiriac, L.B.; Martin, F.; Simon, S. Novel nutraceutical Myricetin composite of enhanced dissolution obtained by co-crystallization with acetamide. *Compos. Part B* **2016**, *89*, 60–66. [[CrossRef](#)]
63. Sowa, M.; Ślepokura, K.; Matczak-Jon, E. Improving solubility of fisetin by cocrystallization. *CrystEngComm* **2014**, *16*, 10592–10601. [[CrossRef](#)]
64. Ren, S.; Liu, M.; Hong, C.; Li, G.; Sun, J.; Wang, J.; Zhang, L.; Xie, Y. The effects of pH, surfactant, ion concentration, coformer, and molecular arrangement on the solubility behavior of myricetin cocrystals. *Acta Pharm. Sin. B* **2018**, *9*, 59–73. [[CrossRef](#)] [[PubMed](#)]
65. Sowa, M.; Ślepokura, K.; Matczak-Jon, E. A 1:1 pharmaceutical cocrystal of myricetin in combination with uncommon piracetam conformer: X-ray single crystal analysis and mechanochemical synthesis. *J. Mol. Struct.* **2014**, *1058*, 114–121. [[CrossRef](#)]
66. Sowa, M.; Ślepokura, K.; Matczak-Jon, E. Cocrystals of fisetin, luteolin and genistein with pyridinecarboxamide cofomers: Crystal structures, analysis of intermolecular interactions, spectral and thermal characterization. *CrystEngComm* **2013**, *15*, 7696–7708. [[CrossRef](#)]
67. Huang, Y.; Zhang, B.; Gao, Y.; Zhang, J.; Shi, L. Baicalein-nicotinamide cocrystal with enhanced solubility, dissolution, and oral bioavailability. *J. Pharm. Sci.* **2014**, *103*, 2330–2337. [[CrossRef](#)]
68. Sowa, M.; Ślepokura, K.; Matczak-Jon, E. A 1:1 cocrystal of baicalein with nicotinamide. *Acta Crystallogr. Sect. C Cryst. Struct. Commun.* **2012**, *68*, o262–o265. [[CrossRef](#)]
69. Zhu, B.; Zhang, Q.; Wang, J.-R.; Mei, X. Cocrystals of Baicalein with Higher Solubility and Enhanced Bioavailability. *Cryst. Growth Des.* **2017**, *17*, 1893–1901. [[CrossRef](#)]
70. Chadha, R.; Bhalla, Y.; Nandan, A.; Chadha, K.; Karan, M. Chrysin cocrystals: Characterization and evaluation. *J. Pharm. Biomed. Anal.* **2017**, *134*, 361–371. [[CrossRef](#)]
71. Sa, R.; Zhang, Y.; Deng, Y.; Huang, Y.; Zhang, M.; Lou, B. Novel Salt Cocrystal of Chrysin with Berberine: Preparation, Characterization, and Oral Bioavailability. *Cryst. Growth Des.* **2018**, *18*, 4724–4730. [[CrossRef](#)]
72. Chadha, K.; Karan, M.; Bhalla, Y.; Chadha, R.; Khullar, S.; Mandal, S.; Vasisht, K. Cocrystals of Hesperetin: Structural, Pharmacokinetic, and Pharmacodynamic Evaluation. *Cryst. Growth Des.* **2017**, *17*, 2386–2405. [[CrossRef](#)]
73. Luo, C.; Liang, W.; Chen, X.; Wang, J.; Deng, Z.; Zhang, H. Pharmaceutical cocrystals of naringenin with improved dissolution performance. *CrystEngComm* **2018**, *20*, 3025. [[CrossRef](#)]
74. Khandavilli, U.B.R.; Skořepová, E.; Sinha, A.S.; Bhogala, B.R.; Maguire, N.M.; Maguire, A.R.; Lawrence, S.E. Cocrystals and a Salt of the Bioactive Flavonoid: Naringenin. *Cryst. Growth Des.* **2018**, *18*, 4571–4577. [[CrossRef](#)]
75. Sowa, M.; Ślepokura, K.; Matczak-Jon, E. A 1:2 cocrystal of genistein with isonicotinamide: Crystal structure and Hirshfeld surface analysis. *Acta Crystallogr. Sect. C Cryst. Struct. Commun.* **2013**, *69*, 1267–1272. [[CrossRef](#)]
76. Zhang, Y.-N.; Yin, H.-M.; Zhang, Y.; Zhang, D.-J.; Su, X.; Kuang, H.-X. Preparation of a 1:1 cocrystal of genistein with 4,4'-bipyridine. *J. Cryst. Growth.* **2017**, *458*, 103–109. [[CrossRef](#)]
77. Sowa, M.; Ślepokura, K.; Matczak-Jon, E. Solid-state characterization and solubility of a genistein–caffeine cocrystal. *J. Mol. Struct.* **2014**, *1076*, 80–88. [[CrossRef](#)]

78. Xu, J.; Huang, Y.; Ruan, S.; Chi, Z.; Qin, K.; Cai, B.; Cai, T. Cocrystals of isoliquiritigenin with enhanced pharmacokinetic performance. *CrystEngComm* **2016**, *18*, 8776–8786. [[CrossRef](#)]
79. Huang, S.; Xu, J.; Peng, Y.; Guo, M.; Cai, T. Facile Tuning of the Photoluminescence and Dissolution Properties of Phloretin through Cocrystallization. *Cryst. Growth Des.* **2019**, *19*, 6837–6844. [[CrossRef](#)]
80. Aakeröy, C.B.; Sinha, A.S.; Chopade, P.D.; Desper, J. Halogen bonding or close packing? Examining the structural landscape in a series of Cu(II)-acac complexes. *Dalton Trans.* **2011**, *40*, 12160–12168. [[CrossRef](#)]
81. Sun, C.C. Materials science tetrahedron—A useful tool for pharmaceutical research and development. *J. Pharm. Sci.* **2009**, *98*, 1671–1687. [[CrossRef](#)] [[PubMed](#)]
82. Zhao, J.; Yang, J.; Xie, Y. Improvement strategies for the oral bioavailability of poorly water-soluble flavonoids: An overview. *Int. J. Pharm.* **2019**, *570*, 118642. [[CrossRef](#)] [[PubMed](#)]
83. Spencer, J.P.; Kuhnle, G.G.; Williams, R.J.; Rice-Evans, C. Intracellular metabolism and bioactivity of quercetin and its in vivo metabolites. *Biochem. J.* **2003**, *372*, 173–181. [[CrossRef](#)] [[PubMed](#)]
84. Leopoldini, M.; Russo, N.; Chiodo, S.; Toscano, M. Iron chelation by the powerful antioxidant flavonoid quercetin. *J. Agric. Food Chem.* **2006**, *54*, 6343–6351. [[CrossRef](#)] [[PubMed](#)]
85. Murakami, A.; Ashida, H.; Terao, J. Multitargeted cancer prevention by quercetin. *Cancer Lett.* **2008**, *269*, 315–325. [[CrossRef](#)]
86. Formica, J.V.; Regelson, W. Review of the biology of Quercetin and related bioflavonoids. *Food Chem. Toxicol.* **1995**, *33*, 1061–1080. [[CrossRef](#)]
87. Vargas, A.J.; Burd, R. Hormesis and synergy: Pathways and mechanisms of quercetin in cancer prevention and management. *Nutr. Rev.* **2010**, *68*, 418–428. [[CrossRef](#)]
88. Reyes-Farias, M.; Carrasco-Pozo, C. The Anti-Cancer Effect of Quercetin: Molecular Implications in Cancer Metabolism. *Int. J. Mol. Sci.* **2019**, *20*, 3177. [[CrossRef](#)]
89. Ader, P.; Wessmann, A.; Wolffram, S. Bioavailability and metabolism of the flavonol quercetin in the pig. *Free Radic. Biol. Med.* **2000**, *28*, 1056–1067. [[CrossRef](#)]
90. Erlund, I.; Freese, R.; Marniemi, J.; Hakala, P.; Alfthan, G. Bioavailability of quercetin from berries and the diet. *Nutr. Cancer* **2006**, *54*, 13–17. [[CrossRef](#)]
91. Hollman, P.C.; van Trijp, J.M.; Buysman, M.N.; van der Gaag, M.S.; Mengelers, M.J.; de Vries, J.H.; Katan, M.B. Relative bioavailability of the antioxidant flavonoid quercetin from various foods in man. *FEBS Lett.* **1997**, *418*, 152–156. [[CrossRef](#)]
92. Lesser, S.; Cermak, R.; Wolffram, S. Bioavailability of quercetin in pigs is influenced by the dietary fat content. *J. Nutr.* **2004**, *134*, 1508–1511. [[CrossRef](#)]
93. Manach, C.; Texier, O.; Morand, C.; Crespy, V.; Régéat, F.; Demigné, C.; Rémésy, C. Comparison of the bioavailability of quercetin and catechin in rats. *Free Radical Biol. Med.* **1999**, *27*, 1259–1266. [[CrossRef](#)]
94. Dabeek, W.M.; Marra, M.V. Dietary Quercetin and Kaempferol: Bioavailability and Potential Cardiovascular-Related Bioactivity in Humans. *Nutrients* **2019**, *11*, 2282. [[CrossRef](#)]
95. Chen, F.; Zhuang, M.; Peng, J.; Wang, X.; Huang, T.; Li, S.; Lin, M.; Lin, H.; Xu, Y.; Li, J.; et al. Baicalein inhibits migration and invasion of gastric cancer cells through suppression of the TGF-beta signaling pathway. *Mol. Med. Rep.* **2014**, *10*, 1999–2003. [[CrossRef](#)]
96. Aryal, P.; Kim, K.; Park, P.H.; Ham, S.; Cho, J.; Song, K. Baicalein induces autophagic cell death through AMPK/ULK1 activation and downregulation of mTORC1 complex components in human cancer cells. *FEBS J.* **2014**, *281*, 4644–4658. [[CrossRef](#)]
97. Lee, H.; Bae, S.; Kim, K.; Kim, W.; Chung, S.I.; Yoon, Y. Beta-Catenin mediates the anti-adipogenic effect of baicalin. *Biochem. Biophys. Res. Commun.* **2010**, *398*, 741–746. [[CrossRef](#)]
98. Li-Weber, M. New therapeutic aspects of flavones: The anticancer properties of *Scutellaria* and its main active constituents Wogonin, Baicalein and Baicalin. *Cancer Treat. Rev.* **2009**, *35*, 57–68. [[CrossRef](#)]
99. Wang, Q.; Wang, Y.T.; Pu, S.P.; Zheng, Y.T. Zinc coupling potentiates anti-HIV-1 activity of baicalin. *Biochem. Biophys. Res. Commun.* **2004**, *324*, 605–610. [[CrossRef](#)]
100. Hong, T.; Jin, G.B.; Cho, S.; Cyong, J.C. Evaluation of the anti-inflammatory effect of baicalein on dextran sulfate sodium-induced colitis in mice. *Planta Med.* **2002**, *68*, 268–271. [[CrossRef](#)]
101. Tuli, H.S.; Aggarwal, V.; Kaur, J.; Aggarwal, D.; Parashar, G.; Parashar, N.C.; Tuorkey, M.; Kaur, G.; Savla, R.; Sak, K.; et al. Baicalein: A metabolite with promising antineoplastic activity. *Life Sci.* **2020**, *259*, 118183. [[CrossRef](#)] [[PubMed](#)]
102. Das, B.K.; Al-Amin, M.M.; Russel, S.M.; Kabir, S.; Bhattacharjee, R.; Hannan, J.M. Phytochemical Screening and Evaluation of Analgesic Activity of *Oroxylum indicum*. *Indian J. Pharm. Sci.* **2014**, *76*, 571–575. [[PubMed](#)]
103. Pi, J.; Wang, S.; Li, W.; Kebebe, D.; Zhang, Y.; Zhang, B.; Qi, D.; Guo, P.; Li, N.; Liu, Z. A nano-cocrystal strategy to improve the dissolution rate and oral bioavailability of baicalein. *Asian J. Pharm. Sci.* **2019**, *14*, 154–164. [[CrossRef](#)] [[PubMed](#)]
104. Zhang, Y.; Luo, R.; Chen, Y.; Ke, X.; Hu, D.; Han, M. Application of carrier and plasticizer to improve the dissolution and bioavailability of poorly water-soluble baicalein by hot melt extrusion. *AAPS PharmSciTech* **2014**, *15*, 560–568. [[CrossRef](#)] [[PubMed](#)]
105. Ashrafizadeh, M.; Tavakol, S.; Ahmadi, Z.; Roomiani, S.; Mohammadinejad, R.; Samarghandian, S. Therapeutic effects of kaempferol affecting autophagy and endoplasmic reticulum stress. *Phytother. Res.* **2020**, *34*, 911–923. [[CrossRef](#)] [[PubMed](#)]
106. Alam, W.; Khan, H.; Shah, M.A.; Cauli, O.; Saso, L. Kaempferol as a Dietary Anti-Inflammatory Agent: Current Therapeutic Standing. *Molecules* **2020**, *25*, 4073. [[CrossRef](#)]

107. Wong, S.K.; Chin, K.Y.; Ima-Nirwana, S. The Osteoprotective Effects of Kaempferol: The Evidence From In Vivo And In Vitro Studies. *Drug Des., Dev. Ther.* **2019**, *13*, 3497–3514. [[CrossRef](#)]
108. Wang, X.; Yang, Y.; An, Y.; Fang, G. The mechanism of anticancer action and potential clinical use of kaempferol in the treatment of breast cancer. *Biomed. Pharmacother.* **2019**, *117*, 109086. [[CrossRef](#)]
109. Imran, M.; Salehi, B.; Sharifi-Rad, J.; Aslam Gondal, T.; Saeed, F.; Imran, A.; Shahbaz, M.; Tsouh Fokou, P.V.; Umair Arshad, M.; Khan, H.; et al. Kaempferol: A Key Emphasis to Its Anticancer Potential. *Molecules* **2019**, *24*, 2277. [[CrossRef](#)]
110. Imran, M.; Rauf, A.; Shah, Z.A.; Saeed, F.; Imran, A.; Arshad, M.U.; Ahmad, B.; Bawazeer, S.; Atif, M.; Peters, D.G.; et al. Chemo-preventive and therapeutic effect of the dietary flavonoid kaempferol: A comprehensive review. *Phytother. Res.* **2019**, *33*, 263–275. [[CrossRef](#)]
111. Devi, K.P.; Malar, D.S.; Nabavi, S.F.; Sureda, A.; Xiao, J.; Nabavi, S.M.; Daglia, M. Kaempferol and inflammation: From chemistry to medicine. *Pharmacol. Res.* **2015**, *99*, 1–10. [[CrossRef](#)]
112. Colombo, M.; de Lima Melchiades, G.; Michels, L.R.; Figueiró, F.; Bassani, V.L.; Teixeira, H.F.; Koester, L.S. Solid Dispersion of Kaempferol: Formulation Development, Characterization, and Oral Bioavailability Assessment. *AAPS PharmSciTech* **2019**, *20*, 106. [[CrossRef](#)]
113. Qian, Y.S.; Ramamurthy, S.; Candasamy, M.; Shadab, M.; Kumar, R.H.; Meka, V.S. Production, Characterization and Evaluation of Kaempferol Nanosuspension for Improving Oral Bioavailability. *Curr. Pharm. Biotechnol.* **2016**, *17*, 549–555. [[CrossRef](#)]
114. Wu, Z.; Li, C.; Chen, Y.; Liu, Q.; Li, N.; He, X.; Li, W.; Shen, R.; Li, L.; Wei, C.; et al. Chrysin Protects Against Titanium Particle-Induced Osteolysis by Attenuating Osteoclast Formation and Function by Inhibiting NF- $\kappa$ B and MAPK Signaling. *Front. Pharmacol.* **2022**, *13*, 793087. [[CrossRef](#)]
115. Geng, A.; Xu, S.; Yao, Y.; Qian, Z.; Wang, X.; Sun, J.; Zhang, J.; Shi, F.; Chen, Z.; Zhang, W.; et al. Chrysin impairs genomic stability by suppressing DNA double-strand break repair in breast cancer cells. *Cell cycle* **2022**, *21*, 379–391. [[CrossRef](#)]
116. Dewi, R.M.; Megawati, M.; Antika, L.D. Antidiabetic Properties of Dietary Chrysin: A Cellular Mechanism Review. *Mini-Rev. Med. Chem.* **2022**, *22*, 1450–1457. [[CrossRef](#)]
117. Khan, A.; Ikram, M.; Hahm, J.R.; Kim, M.O. Antioxidant and Anti-Inflammatory Effects of Citrus Flavonoid Hesperetin: Special Focus on Neurological Disorders. *Antioxidants* **2020**, *9*, 609. [[CrossRef](#)]
118. Jin, Y.R.; Han, X.H.; Zhang, Y.H.; Lee, J.J.; Lim, Y.; Chung, J.H.; Yun, Y.P. Antiplatelet activity of hesperetin, a bioflavonoid, is mainly mediated by inhibition of PLC-gamma2 phosphorylation and cyclooxygenase-1 activity. *Atherosclerosis* **2007**, *194*, 144–152. [[CrossRef](#)]
119. Wang, Y.; Liu, S.; Dong, W.; Qu, X.; Huang, C.; Yan, T.; Du, J. Combination of hesperetin and platinum enhances anticancer effect on lung adenocarcinoma. *Biomed. Pharmacother.* **2019**, *113*, 108779. [[CrossRef](#)]
120. Ersoz, M.; Erdemir, A.; Duranoglu, D.; Uzunoglu, D.; Arasoglu, T.; Derman, S.; Mansuroglu, B. Comparative evaluation of hesperetin loaded nanoparticles for anticancer activity against C6 glioma cancer cells. *Artif. Cells Nanomed., Biotechnol.* **2019**, *47*, 319–329. [[CrossRef](#)]
121. Kim, H.W.; Woo, H.J.; Yang, J.Y. Hesperetin Inhibits Expression of Virulence Factors and Growth of Helicobacter pylori. *Int. J. Mol. Sci.* **2021**, *22*, 10035. [[CrossRef](#)] [[PubMed](#)]
122. Muhammad, T.; Ikram, M.; Ullah, R.; Rehman, S.U.; Kim, M.O. Hesperetin, a Citrus Flavonoid, Attenuates LPS-Induced Neuroinflammation, Apoptosis and Memory Impairments by Modulating TLR4/NF- $\kappa$ B Signaling. *Nutrients* **2019**, *11*, 648. [[CrossRef](#)] [[PubMed](#)]
123. Yap, K.M.; Sekar, M.; Wu, Y.S.; Gan, S.H.; Rani, N.; Seow, L.J.; Subramaniyan, V.; Fuloria, N.K.; Fuloria, S.; Lum, P.T. Hesperidin and its aglycone hesperetin in breast cancer therapy: A review of recent developments and future prospects. *Saudi J. Biol. Sci.* **2021**, *28*, 6730–6747. [[CrossRef](#)] [[PubMed](#)]
124. Oo, A.; Hassandarvish, P.; Chin, S.P.; Lee, V.S. In silico study on anti-Chikungunya virus activity of hesperetin. *PeerJ* **2016**, *4*, e2602. [[CrossRef](#)] [[PubMed](#)]
125. Yang, G.; Yin, X.; Ma, D.; Su, Z. Anticancer activity of Phloretin against the human oral cancer cells is due to G0/G1 cell cycle arrest and ROS mediated cell death. *J. BUON* **2020**, *25*, 344–349.
126. Anunciato Casarini, T.P.; Frank, L.A.; Pohlmann, A.R.; Guterres, S.S. Dermatological applications of the flavonoid phloretin. *Eur. J. Pharmacol.* **2020**, *889*, 173593. [[CrossRef](#)]
127. Wu, M.; Li, P.; An, Y.; Ren, J.; Yan, D.; Cui, J.; Li, D.; Li, M.; Wang, M.; Zhong, G. Phloretin ameliorates dextran sulfate sodium-induced ulcerative colitis in mice by regulating the gut microbiota. *Pharmacol. Res.* **2019**, *150*, 104489. [[CrossRef](#)]
128. Liu, N.; Zhang, N.; Zhang, S.; Zhang, L.; Liu, Q. Phloretin inhibited the pathogenicity and virulence factors against *Candida albicans*. *Bioengineered* **2021**, *12*, 2420–2431. [[CrossRef](#)]
129. Kim, U.; Kim, C.Y.; Lee, J.M.; Oh, H.; Ryu, B.; Kim, J.; Park, J.H. Phloretin Inhibits the Human Prostate Cancer Cells Through the Generation of Reactive Oxygen Species. *Pathol. Oncol. Res.* **2020**, *26*, 977–984. [[CrossRef](#)]
130. Lin, S.C.; Chen, M.C.; Liu, S.; Callahan, V.M.; Bracci, N.R.; Lehman, C.W.; Dahal, B.; de la Fuente, C.L.; Lin, C.C.; Wang, T.T.; et al. Phloretin inhibits Zika virus infection by interfering with cellular glucose utilisation. *Int. J. Antimicrob. Agents* **2019**, *54*, 80–84. [[CrossRef](#)]

131. Dierckx, T.; Haidar, M.; Grajchen, E.; Wouters, E.; Vanherle, S.; Loix, M.; Boeykens, A.; Bylemans, D.; Hardonnière, K.; Kerdine-Römer, S.; et al. Phloretin suppresses neuroinflammation by autophagy-mediated Nrf2 activation in macrophages. *J. Neuroinflammation* **2021**, *18*, 148. [[CrossRef](#)]
132. Singh, G.; Thaker, R.; Sharma, A.; Parmar, D. Therapeutic effects of biochanin A, phloretin, and epigallocatechin-3-gallate in reducing oxidative stress in arsenic-intoxicated mice. *Environ. Sci. Pollut. Res.* **2021**, *28*, 20517–20536. [[CrossRef](#)]

**Disclaimer/Publisher’s Note:** The statements, opinions and data contained in all publications are solely those of the individual author(s) and contributor(s) and not of MDPI and/or the editor(s). MDPI and/or the editor(s) disclaim responsibility for any injury to people or property resulting from any ideas, methods, instructions or products referred to in the content.